16th World Conference on Earthquake, 16WCEE 2017
Santiago Chile, January 9th to 13th 2017
Paper N° 4610 (Abstract ID)
Registration Code: S-XXXXXXXX

Probabilistic Seismic Damage Analysis of Buildings using Damage Scenarios

E. Tahmasebi[(1)], R. Sause[(2)], J. M. Ricles[(3)]

[(1)] *Postdoctoral Research Associate, Lehigh University, tahmasebi@lehigh.edu*
[(2)] *Professor of Structural Engineering, Lehigh University, rs0c@lehigh.edu*
[(3)] *Professor of Structural Engineering, Lehigh University, jmr5@lehigh.edu*
...

Abstract

In this paper the seismic damage analysis of a building at the system level, subsystem level, and component level is organized into a damage scenario tree. Damage scenarios involving building collapse, building demolition and reconstruction, and component damage are defined. Damage scenario tree analysis provides a rigorous framework for calculating the fragilities for various damage scenarios. Probabilities of different damage scenarios are evaluated for treating earthquake ground motion variability. Engineering demand parameter (EDP)-based and hazard intensity measure (IM)-based methods are used for quantifying the probability of damage scenarios. Variability in structural response due to variation of ground motion records are included on a record-by-record basis. Applications to a 9-story special concentrically braced frame office building are shown. Damage scenario fragilities are developed using damage scenario tree analysis procedure.

.Keywords: damage scenario; collapse; demolition; probabilistic damage analysis

1 Introduction

Seismic performance analysis of a building can be organized into four stages: (i) hazard analysis; (ii) structural response analysis; (iii) damage analysis; and (iv) loss estimation. This analysis process involves distinct categories of random variables, including: hazard intensity measures (IM), engineering demand parameters (EDP), damage measures, and decision variables [1, 2, 3]. The results from the structural response analysis and the damage analysis are used in the loss estimation for the building.

Structural collapse of a building is a major contributor to the estimated earthquake-induced loss for the building. The seismic collapse capacity of a building is usually estimated using incremental dynamic analysis (IDA) results [4]. An IDA consists of nonlinear structural response history analyses performed for a ground motion record as the ground motion intensity is increased incrementally. The usual IDA procedure is to conduct structural response analyses at increasing seismic hazard intensities for a set of ground motions [5]. Building collapse capacity is then determined as the seismic hazard intensity at which the building becomes unstable and unable to carry seismic lateral forces.

In addition to collapse, structural damage which does not cause the building to collapse, but results in significant permanent (residual) deformation, is a second major contributor to the estimated loss [3], because buildings with significant residual deformations are often demolished rather than repaired [6, 7]. The amplitude of the residual deformation (e.g., the residual story drift ratio) is an important indicator of damage. Increased inelastic deformation in structural components increase the likelihood of residual deformation [8, 9, 10, 11, 12, 13, 14].

Previous research has considered the consequences of residual story drift. For example, Uma et al. [15] use the joint distribution of the maximum story drift ratio and the residual story drift ratio to provide a three-dimensional performance matrix. Ramirez and Miranda [3] developed a loss estimation procedure that includes the residual story drift ratio and the resulting probability of demolition in the total estimated loss.

This paper presents a framework for probabilistic seismic damage analysis of buildings by including damage assessments at the system level, subsystem level, and component level, consistent with the seismic performance assessment methodology of FEMA P-58 [16]. A damage scenario tree analysis technique is used to evaluate the probability of different damage scenarios at varying seismic hazard intensities. The result from IDA is used for the system level, subsystem level, and component level damage assessments. Damage scenarios are defined using a damage scenario tree and the mathematical formulation for the probability of each damage scenario is presented. Epistemic uncertainty regarding the damage state criteria and record-to-record variability in structural response are considered in estimating the damage scenario probabilities. Combination of EDP-based and IM-based methods are used for evaluation of probability of different damage scenarios. The probability of occurrence for the damage scenarios are estimated for an example building structure.

2 Damage Scenario Tree Analysis

2.1 Damage scenario tree

A quantitative probabilistic study of a sequence of events resulting from an initiating event can be performed using an event tree analysis (ETA) [17]. In the present study, the ETA technique is adapted to develop a so-called damage scenario tree analysis (DSTA) of the seismic damage to a building, consistent with the proposed methodology of FEMA P-58 [16]. A DSTA uses a hierarchy of levels: (i) the entire system (i.e., the building); (ii) subsystems (e.g., the seismic lateral force resisting system of the building); and (iii) components (e.g., structural components such as columns, braces, and beams, or non-structural components such as cladding and partition walls). Fig. 1 shows a general damage scenario tree diagram.

The initiating event (IE) for an ETA is usually an undesirable event that has consequences leading to an end state. In a DSTA, the hypothetical occurrence of an earthquake ground motion at the building site, at a given IM value, is treated as the IE for the seismic damage analysis of the building.

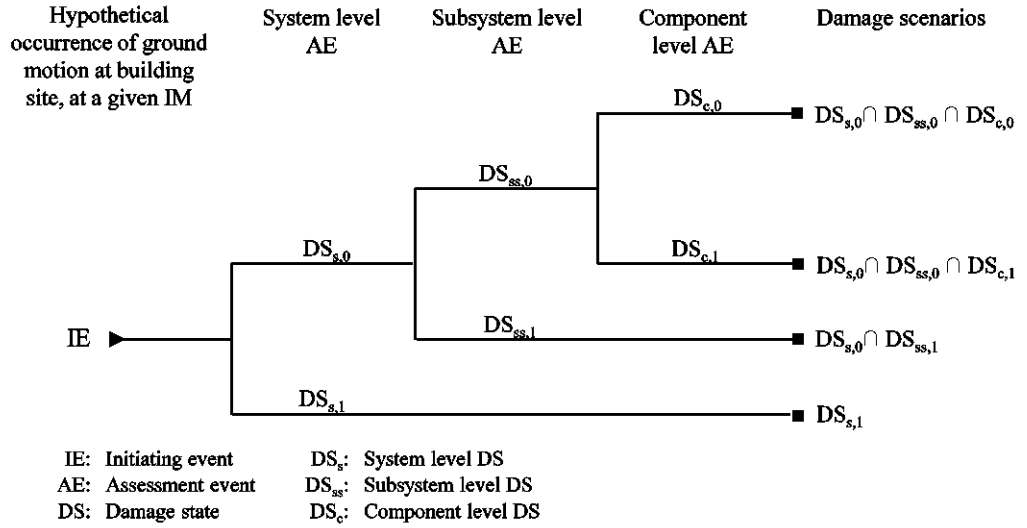

Fig. 1 Organization of damage analysis for building at system, subsystem, and component levels using damage scenario tree

In an ETA, pivotal events (PE) are the events that may follow from the IE [17]. In a DSTA, the PE are a sequence of assessment events (AE) at the system level, subsystem level, and component level of the building. Each AE is a probabilistic assessment of the damage state (DS) for the system, a subsystem, or a component.

Each AE has two or more resulting DS which form different branches of the damage scenario tree. The DS considered at each AE must be mutually exclusive and collectively exhaustive. This guarantees that the state of the system, a subsystem, or a component under assessment is definitely described by only one DS. A path from the IE to the end of a branch, including all the DS along the path, is called a damage scenario. Different damage scenarios are shown as the intersection of the DS along the path to a branch end in Fig. 1.The state of no damage at the system level, subsystem level, and component level are described by $DS_{s,0}$, $DS_{ss,0}$, or $DS_{c,0}$, respectively, in Fig. 1.

The DS are described qualitatively in terms of the repair action (RA) required to restore the system, subsystem, or component back to an acceptable (e.g., functional) state. A one-to-one correspondence between a DS and the corresponding RA is established, where the RA is used to describe the DS. The probability of being in a DS is assessed quantitatively using one or more related EDPs, obtained from structural response analysis. Each

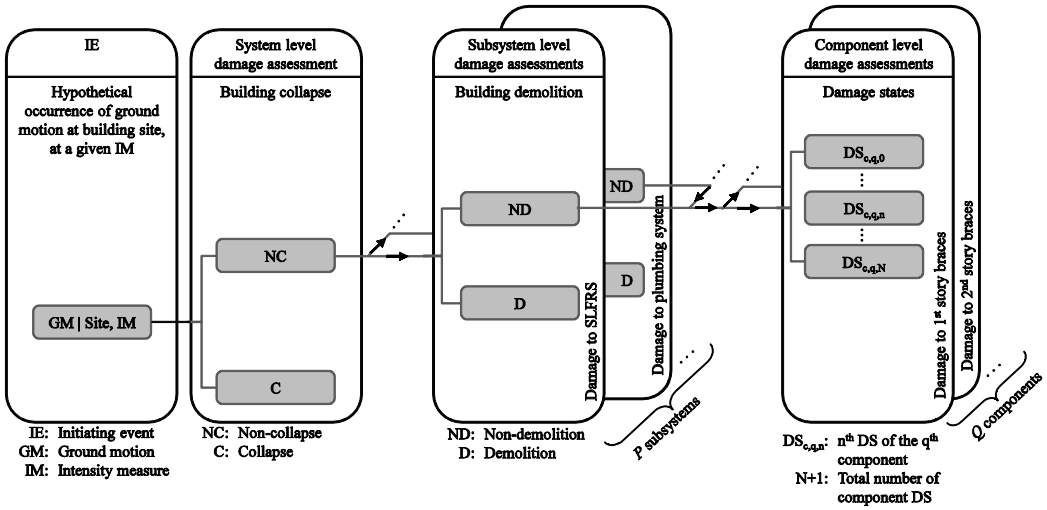

Fig. 2 Damage scenario tree diagram for probabilistic damage analysis of building

EDP is a random variable. Details about the EDPs and the uncertainties contributing to the randomness of the EDPs are given later.

Fig. 2 shows that the system level DS of the building are "non-collapse", $DS_{s,0} = NC$, and "collapse", $DS_{s,1} = C$, of the building. The corresponding RA for non-collapse is to conduct repairs indicated by the subsystem and component DS. The corresponding RA for collapse is to remove the debris and reconstruct the building.

The damage to a subsystem (such as the seismic lateral force resisting system (SLFRS) or the plumbing system) of the building is described using the RA of non-demolition (ND), and demolition and reconstruction (D) of the building corresponding to $DS_{ss,0}$ and $DS_{ss,1}$, respectively, in Fig. 1. ND and D were selected as the subsystem-level RA, assuming that it is not feasible to repair a building with a heavily damaged subsystem (see Fig. 2). Any subsystem that can be damaged to an extent that could lead to demolition and reconstruction of the building could be considered.

The damage to each component can be quantified by different DS, described by the corresponding RA. The identified DS for each component must be mutually exclusive and cover all possible states of the component (i.e., be collectively exhaustive). Fig. 2 shows N+1 possible damage states for a component level damage assessment.

2.2 Quantifying building collapse

Building collapse (C) is a damage scenarios from the damage scenario tree shown in Fig. 2. It involves only the system level damage assessment as the subsystem level and component level damage assessment are irrelevant when the building collapses. Probability of building collapse is often quantified using a ground motion hazard intensity measure (denoted by IM) value [4]. The 5% damped spectral acceleration at the fundamental period of the building, $S_a(T, 5\%)$, is a common IM used for quantifying the probability of building collapse. Using this IM-based method, the probability of collapse for the building subjected to an individual ground motion record (e.g., the l^{th} ground motion record, denoted by GM_l) at a given $IM = im$ value is evaluated as follows:

$$P(C|IM = im, GM_l) = P(IM \geq IM_C|IM = im, GM_l) = F_{IM_{C,l}}(im) \quad (1)$$

where GM_l is an individual ground motion record, IM_C is the IM value at which collapse occurs, defined as a random variable, and $F_{IM_{C,l}}$ is the cumulative distribution function (CDF) of the IM_C, also known as the collapse fragility function for GM_l. For the building under consideration, F_{IM_C} is determined for individual ground motion records and therefore varies from ground motion record to ground motion record.

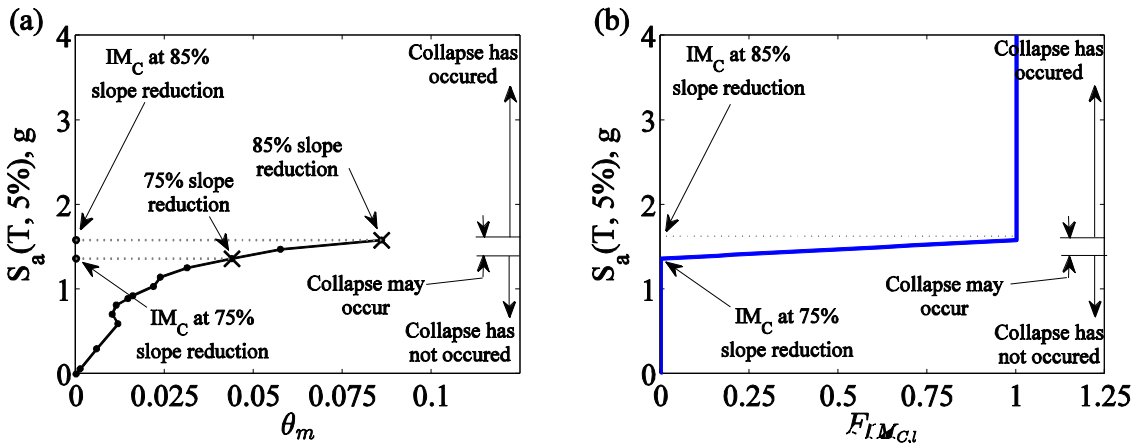

Fig. 3 IM-based method of quantifying collapse DS probability for a given GM_l with epistemic uncertainty in collapse DS criteria: (a) IDA for an individual ground motion record GM_l; and (b) probability of collapse for GM_l(i.e., $F_{IM_{C,l}}$)

The epistemic uncertainty in IM_c for GM_l, i.e., the collapse DS criteria for GM_l, is represented in $F_{IM_{C,l}}$. This epistemic uncertainty in collapse DS criteria is due to the lack of knowledge about the IM value at which the building collapses, which could be from different sources such as approximate modeling of various deteriorating mechanisms in the SLFRS of the building or selecting the flattening point on an IDA curve as the collapse point. Fig. 3 shows the effect of uncertainty in selecting a point at which the IDA curve flattens as the collapse point. Three regions are specified along the $S_a(T, 5\%)$ axis (i.e., IM axis) of Fig. 3(a): (i) IM values for which collapse has not occurred; (ii) IM values for which collapse may occur; and (iii) IM values for which collapse has occurred. Two values of slope reduction (i.e., flattening) of the IDA curve are considered for separating the three ranges of IM value, 75% and 85%. The 75% and 85% slope reduction values are reduction in the tangent slope of the IDA curve, measured with respect to the median of initial slopes of elastic IDA curves for the ground motion record set as specified in FEMA 355F [18]. It is assumed that the distribution of IM_C is uniform across the IM range that collapse may occur. As a result, the collapse fragility function $F_{IM_{C,l}}$ has a ramp shape which start from zero at IM value corresponding to 75% slope reduction and increases linearly to 1 at IM value corresponding to 85% slope reduction as shown in Fig. 3(b).

2.3 Quantifying damage using EDP

Engineering demand parameters (EDP) such as maximum story drift ratio, residual deformation in braces, etc. can be used to quantify the probability of being in a DS at the subsystem level and component level damage assessment. The EDP values are obtained from response history analyses of the building. The EDPs corresponding to the subsystem level and component level damage assessments are denoted by EDP_{ss} and EDP_c, respectively. EDP_{ss}, and EDP_c are random variables. Three primary sources of uncertainty in these EDP values are: (i) the ground motion record-to-record (RTR) variability of the structural response; (ii) the variability of the building system parameters; and (iii) the uncertainty regarding the model of the building (e.g., modeling decisions and parameters) used in the nonlinear structural response analyses.

For a specific subsystem, among all P subsystems considered in the DSTA (shown in Fig. 2), the corresponding EDP is denoted by $EDP_{ss.p}$, where the subscript p indicates the p^{th} subsystem. Similarly, for a specific component, among all Q components considered in the DSTA (shown in Fig. 2), the corresponding EDP is denoted by $EDP_{c.q}$, where the subscript q indicates the q^{th} component.

An EDP limit value (denoted by $EDP_{DS,i}$) is used to distinguish between the $(i-1)^{th}$ DS and i^{th} DS for the system, for a subsystem, or for a component. The EDP limit values for the subsystem level, and component level damage assessment are denoted by $EDP_{ss,p,DS,nss}$, and $EDP_{c,q,DS,n}$, respectively. As stated previously, indices p and q indicate the p^{th} subsystem and q^{th} component, respectively. The indices $nss = \{0,1,\cdots,Nss\}$ and $n = \{0,1,\cdots,N\}$ specify the DS number for the subsystem level and component level damage assessments, respectively. As shown in Fig. 2, one EDP limit value is required to separate the two DS of non-collapse and collapse at the system level (i.e., $Ns = 1$).

As shown in Fig. 2 one EDP limit value is required to separate the two DS of non-demolition and demolition at the subsystem level (i.e., $Nss = 1$). The EDP limit value separating the non-demolition from the demolition is $EDP_{ss,p,DS,1} = EDP_{ss,p,D}$, where the subscript D stands for demolition. At the component level, N EDP limit values are required to separate the $N+1$ damage state. The first component level DS, denoted by $DS_{c,q,0}$ (see Fig. 2), is the state of having no damage with no required repair action.

The present study considers only the SLFRS subsystem in the damage analysis (i.e., $P = 1$). The maximum (over all stories of the building) residual story drift ratio, θ_r, is used as the subsystem level EDP (i.e., $EDP_{ss} = \theta_r$) for the SLFRS subsystem [3]. The θ_r limit value, separating the non-demolition DS from the demolition DS, is $EDP_{ss,1,D} = \theta_{r,D}$. Later in the paper, where DSTA is applied to the 9-story special concentrically braced frame (SCBF) building, examples of $EDP_{c,q}$ and $EDP_{c,q,DS,n}$ are given.

Recognizing the epistemic uncertainty in the damage state criteria, the EDP limit values (i.e., $EDP_{ss,1,D} = \theta_{r,D}$, and $EDP_{c,q,DS,n}$) are also treated as random variables (rather than deterministic limit values). In other words, the EDP limit values are treated as random variables due to a lack of knowledge of the precise value of an EDP

separating two DS. For example, the precise value of θ_r separating the non-demolition DS from the demolition DS is uncertain. Probability distributions for the EDP limit values can be estimated from analytical work, published test data, and post-earthquake reconnaissance reports [2, 16]. The probability of a given EDP value ($EDP = edp$) exceeding an EDP limit value, $EDP_{DS,i}$, is quantified by evaluating the cumulative density function (CDF) of $EDP_{DS,i}$ at edp as follows:

$$P\left(EDP \geq EDP_{DS,i} \middle| EDP = edp\right) = F_{EDP_{DS,i}}(edp) \tag{2}$$

where edp is a value of the EDP, $EDP_{DS,i}$ is the i^{th} EDP limit value separating the $(i-1)^{th}$ DS from the i^{th} DS, and $F_{EDP_{DS,i}}$ is the CDF for $EDP_{DS,i}$ which is the i^{th} EDP limit value fragility function. For example, for the SLFRS subsystem level damage assessment, the demolition fragility function is denoted by $F_{\theta_{r,D}}$.

2.4 Damage scenario probability

The probability occurrence of each damage scenario is equal to the probability of intersection of the damage states which form the damage scenario (see Fig. 1). Three damage scenarios from the damage tree of Fig. 2 at a given IM value are: (i) collapse ($C|IM$); (ii) non-collapse with demolition ($NC \cap D|IM$); and (iii) non-collapse, non-demolition, with component damage ($NC \cap ND \cap DS_{c,q,n}|IM$). Probability of building collapse at a given IM value for an individual ground motion record GM_l is given by Eq. (1). Probability of non-collapse with demolition at a given IM value for an individual ground motion record GM_l is as follows:

$$P(NC \cap D|IM = im, GM_l) = P\left(IM < IM_C \cap \theta_r \geq \theta_{r,D} \middle| IM = im, GM_l\right) = \bar{F}_{IM_{C,l}}(im) \cdot F_{\theta_{r,D}}(\theta_{r,l}) \tag{3}$$

where $\bar{F}_{IM_{C,l}} = 1 - F_{IM_{C,l}}$ is the complement of collapse fragility function for GM_l and $\theta_{r,l}$ is the θ_r value obtained from the structural response history analysis of the building subjected to GM_l at $IM = im$. In writing Eq. (3) it is assumed that IM_C and $\theta_{r,D}$ are statistically independent.

Similarly, probability of non-collapse, non-demolition, with component damage at a given IM value for an individual ground motion record GM_l is as follows:

$$\begin{aligned} &P\left(NC \cap ND \cap DS_{c,q,n} \middle| IM = im, GM_l\right) \\ &\quad = \bar{F}_{IM_{C,l}}(im) \cdot \bar{F}_{\theta_{r,D}}\left(\theta_{r,l}\right) \cdot \left(F_{EDP_{c,q,DS,n}}\left(EDP_{(c,q)_l}\right) - F_{EDP_{c,q,DS,n}}\left(EDP_{(c,q)_l}\right)\right) \end{aligned} \tag{4}$$

where $\bar{F}_{\theta_{r,D}} = 1 - F_{\theta_{r,D}}$ is the complement of demolition fragility function for GM_l, $F_{EDP,c,q,DS,n}$ is the general form of a component fragility function for the q^{th} component and n^{th} damage state, and $EDP_{(c,q)_l}$ is the relevant EDP value for the q^{th} component obtained from the structural response history analysis of the building subjected to GM_l at $IM = im$. In writing Eq. (4) it is assumed that IM_C, $\theta_{r,D}$, and $EDP_{c,q,DS,n}$ are statistically independent.

2.5 Including record-to-record variability in structural response

Eq. (1), Eq. (3), and Eq. (4) are written for an individual ground motion record GM_l. Combining the results from structural response history analyses for multiple ground motion records (i.e., a ground motion record set) includes the effect of record-to-record (RTR) variability in structural response in the probability of damage scenarios.

When conducting IDA for a set of ground motion record, damage scenario probabilities can be determined for each ground motion record individually using Eq. (1), Eq. (3), and Eq. (4). IDA is in fact a Monte Carlo simulation [19]. Therefore, probabilities for individual ground motion records can be combined using the law of total probability. In this regard, the collapse damage scenario probabilities for multiple ground motion records can be combined using the law of total probability and Eq. (1) as follows:

$$P(C|IM=im) = \sum_{all\ GM_l} P(C|IM=im, GM_l) \cdot P(GM_l|IM=im) = \sum_{all\ GM_l} F_{IM_{C,l}}(im) \cdot P(GM_l|IM=im) \quad (5)$$

where $P(GM_l|IM=im)$ is the probability of ground motion GM_l scaled to $IM=im$ value. Similarly, the $NC \cap D$ and $NC \cap ND \cap DS_{c,q,n}$ damage scenario probabilities for multiple ground motion records can be combined using the law of total probability and Eq. (3) and Eq. (4) as follows:

$$P(NC \cap D|IM=im) = \sum_{all\ GM_l} P(NC \cap D|IM=im, GM_l) \cdot P(GM_l|IM=im) = \sum_{all\ GM_l} \bar{F}_{IM_{C,l}}(im) \cdot F_{\theta_{r,D}}(\theta_{r,l}) \cdot P(GM_l|IM=im) \quad (6)$$

$$P\left(NC \cap ND \cap DS_{c,q,n}\middle|IM=im\right) = \sum_{all\ GM_l} P\left(NC \cap ND \cap DS_{c,q,n}\middle|IM=im, GM_l\right) \cdot P(GM_l|IM=im) = \sum_{all\ GM_l} \bar{F}_{IM_{C,l}}(im) \cdot \bar{F}_{\theta_{r,D}}(\theta_{r,l}) \cdot \left(F_{EDP_{c,q,DS,n}}\left(EDP_{(c,q)_l}\right) - F_{EDP_{c,q,DS,n}}\left(EDP_{(c,q)_l}\right)\right) \cdot P(GM_l|IM=im) \quad (7)$$

Eq. (5), Eq. (6), and Eq. (7) are derived on a record-by-record basis, i.e., each ground motion record is treated separately when quantifying the damage scenario probabilities.

A common term in Eq. (5), Eq. (6), and Eq. (7) is $P(GM_l|IM=im)$. Note that $\sum_{all\ GM_l} P(GM_l|IM=im)$ must be equal to 1 at all $IM=im$ values following the law of total probability. Eq. (5), Eq. (6), and Eq. (7) are in fact the weighted average of the individual probabilities for individual GM_l. The weights are $P(GM_l|IM=im)$ for each GM_l at a given $IM=im$ value. In the presented example in this study, it is assumed that all ground motion records are equally probable at all $IM=im$ values. However, Eq. (5), Eq. (6), and Eq. (7) allow for using different probabilities for different ground motion records at different $IM=im$ values, in the case of a site-specific ground motion record selection, for instance.

3 Application of Damage Scenario Tree Analysis

3.1 Archetype building and ground motion record set

In the present study, the DSTA is applied to an archetype building. The archetype building is a 9-story building with a special concentrically braced frame (SCBF) SLFRS, located in the Los Angeles area, which is designed according to ASCE 7-10 for seismic design category D_{max} [20].

The typical bracing configuration and story plan of the 9-story SCBF building are shown in Fig. 4. Numerical modeling and nonlinear response analyses were carried out using the OpenSees computational framework [21]. The structural members of the SCBF have wide flange shape cross sections. The Menegotto-Pinto hysteretic model is used for the structural steel material. Inelastic beam-column fiber elements are used to model the structural members. An initial lateral imperfection is introduced at the middle of the braces to initiate global brace buckling [22]. Fracture of the braces due to low-cycle fatigue, induced by local buckling, is modeled using a rainflow cycle counting method [23]. The rigidity of the brace gusset plates at the connections of the braces to the beams and columns are considered in the numerical modeling. The P-Δ effects of the gravity forces in the building are simulated using a lean-on-column.

The ground motion record (GM) set used in this study is the far-field record set from FEMA P695 [4]. The ground motion scaling is done in two steps: (i) the individual GM are "normalized" by their respective peak ground velocities [4]; (ii) the normalized GM are collectively scaled to a specific IM value such that the median IM of the

Table 1 Central value and logarithmic standard deviation of EDP limiting parameter for building demolition and brace damage states Chemical

EDP limit value	Median	Logarithmic std. deviation ($\sigma_{\ln}$)
$\boldsymbol{\theta_{r,D}}$	0.01	0.3
$\boldsymbol{\Delta_{Or,DS,1}}$	0.01	0.25
$\boldsymbol{\Delta_{Or,DS,2}}$	0.025	0.3

scaled record set matches the specific IM value [4]. In the present study IM is the 5% damped spectral acceleration at the approximate fundamental period of the building, $S_a(T, 5\%)$.

3.2 Evaluation of EDP values using IDA

In the present study, an engineering demand parameter (EDP) is a structural response of interest, such as story drift ratio, member deformation, etc. Structural response analyses in the form of IDA [5], are used to estimate the EDP values for a range of IM values. An IDA consists of a set of structural response analyses for one ground motion record (GM_l) as the IM value is increased. The usual IDA procedure is to conduct structural response analyses for a set of ground motion records ($GM_l, l = 1 \cdots L$) scaled to incrementally increasing IM values. EDP values are obtained from the response of the structure to the set of $GM_l, l = 1 \cdots L$ for a given IM, and the resulting EDP values are considered to be conditioned on the IM.

3.3 Damage state fragility functions

As stated previously, the probability of being in a damages state (DS) when conducting an assessment event at system level, subsystem level, and component level is quantified using relevant fragility functions. At the system level damage assessment, the probability of building collapse is quantified using $F_{IM_{C,l}}$ for each individual GM_l, as discussed previously. Probability of damage to the SLFRS of the building that requires the demolition of the building is quantified using the maximum (over all stories) residual story drift ratio, θ_r, and the θ_r limit value for building demolition, $\theta_{r,D}$. It is assumed that $\theta_{r,D}$ follows a lognormal distribution. The median and logarithmic standard deviation values for building demolition fragility function $F_{\theta_{r,D}}$ are given in Table 1 [16]. $F_{\theta_{r,D}}$ is shown in Fig. 5(a).

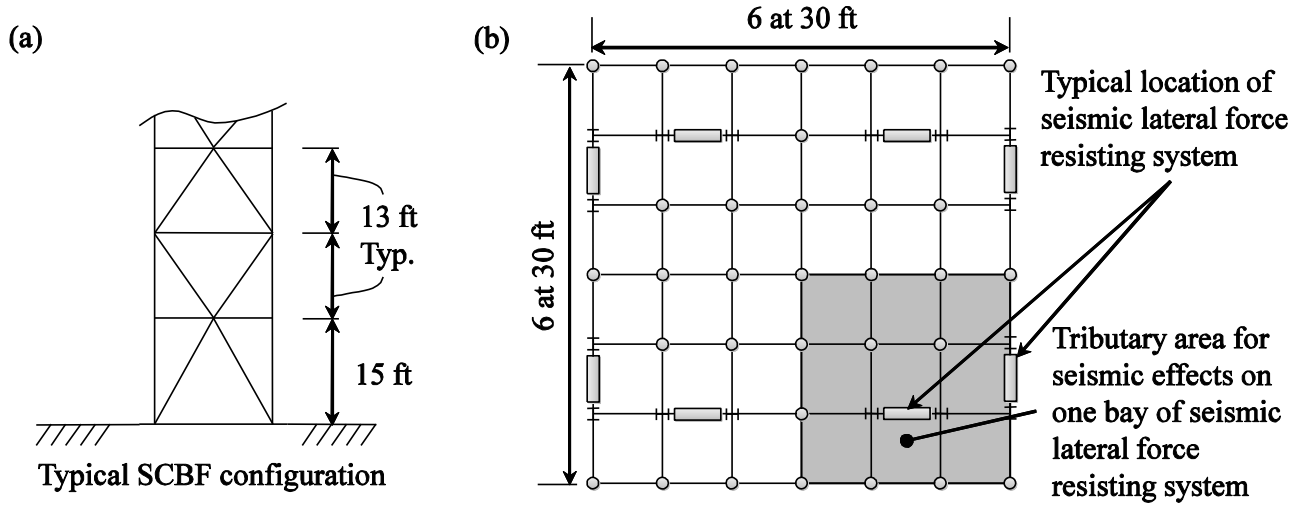

Fig. 4 9-story SCBF building: (a) typical bracing configuration along the height of the building; and (b) typical floor plan and tributary area for seismic effect on one bay SCBF

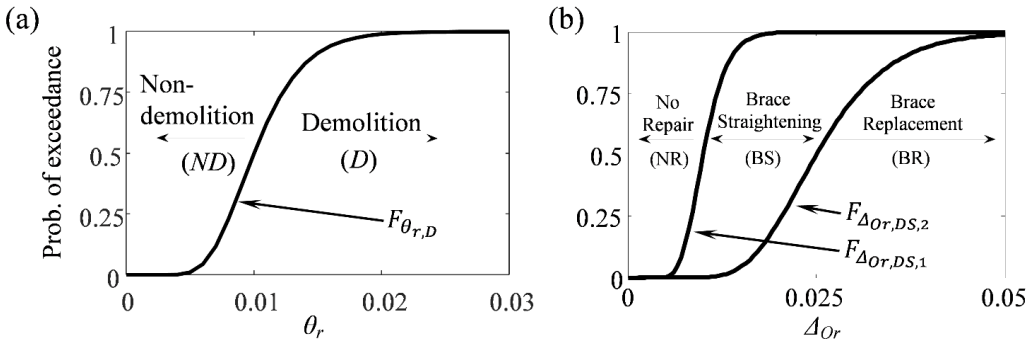

Fig. 5 Damage state fragility functions: (a) demolition fragility function $F_{\theta_{r,D}}$; and (b) brace damage state fragility functions $F_{\Delta_{Or,DS,1}}$ and $F_{\Delta_{Or,DS,2}}$

At the component level damage assessment, the individual brace members of the SCBF are considered. The damage to individual brace members are quantified using the normalized residual out-of-plane deformation of the brace divided by the initial length of the brace, (denoted by Δ_{Or}). Three brace DS with corresponding repair actions of: (i) no repair, NR (corresponds to $DS_{\mathrm{c,q,0}}$); (ii) brace straightening, BS (corresponds to $DS_{\mathrm{c,q,1}}$); and (iii) brace replacement BR (corresponds to $DS_{\mathrm{c,q,2}}$) are considered [24]. These three brace damage states are separated by two Δ_{Or} limit values: $\Delta_{Or,DS,1}$ and $\Delta_{Or,DS,2}$. It is assumed that $\Delta_{Or,DS,1}$ and $\Delta_{Or,DS,2}$ follow lognormal distributions. The median and logarithmic standard deviation values for the brace damage state fragility functions $F_{\Delta_{\mathrm{Or,DS,1}}}$ and $F_{\Delta_{\mathrm{Or,DS,2}}}$ are given in Table 1. These values are selected based on experimental results by Powell [25] and analytical studies by Akbas [24]. $F_{\Delta_{\mathrm{Or,DS,1}}}$ and $F_{\Delta_{\mathrm{Or,DS,2}}}$ are shown in Fig. 5(b).

3.4 Damage scenario fragilities

The fragilities for damage scenarios are developed by evaluating the probability of damage scenarios at various $S_a(T, 5\%)$ values using Eq. (5), Eq. (6), and Eq. (7) and the response history analyses results from IDA. Each GM_l in the ground motion set is assumed to be equally probable at all IM values [19]. Therefore $P(GM = GM_l \mid IM) = 1/L$ where L is the total number of ground motion records in the record set.

The fragility for collapse, (C), and non-collapse with demolition, $(NC \cap D)$, damage scenarios are shown in Fig. 6. As it can be seen from Fig. 6(a), probability of building collapse increases as $S_a(T, 5\%)$ increases. The dispersion of fragility for collapse damage scenario in Fig. 6(a) is from two sources: (i) the RTR variability in

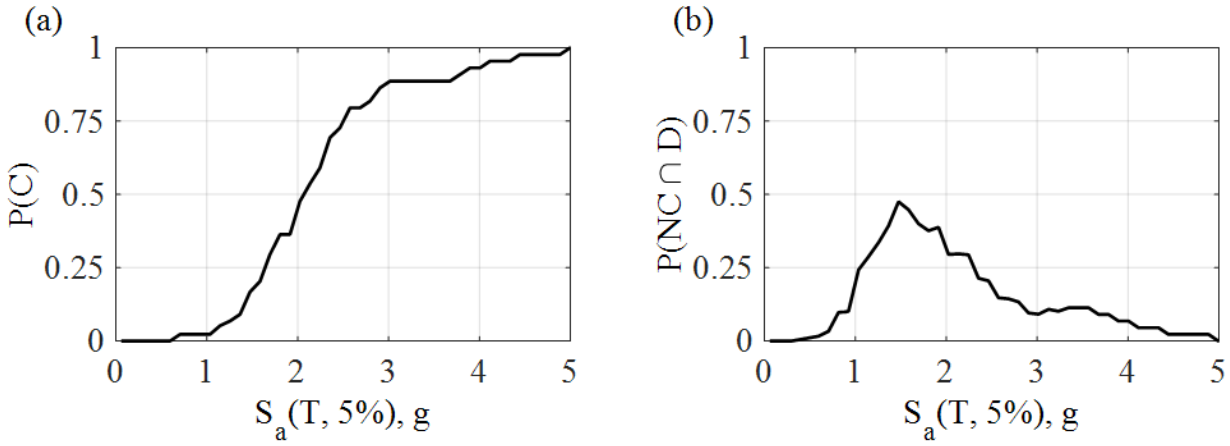

Fig. 6 Damage scenario fragilities for 9-story SCBF building using damage scenario tree analysis: (a) fragility for collapse (C)damage scenario; and (b) fragility for non-collapse with demolition $(NC \cap D)$ damage scenario

structural response; and (ii) the epistemic uncertainty in collapse fragility functions $F_{IM_{C,l}}$. The contribution of the RTR variability in collapse damage state fragility of Fig. 6(a) is considerably greater than the contribution of the epistemic uncertainty in $F_{IM_{C,l}}$.

The fragility for non-collapse with demolition ($NC \cap D$) damage scenario is shown in Fig. 6(b). This fragility is developed by evaluating Eq. (6) at various $S_a(T, 5\%)$ values. It can be seen from Fig. 6(b) that $P(NC \cap D)$ is close to zero at small $S_a(T, 5\%)$ values, increases as $S_a(T, 5\%)$ values increase, reaches a peak value, and finally decreases to zero as $S_a(T, 5\%)$ values decrease. Such a trend of increase and then decrease in $P(NC \cap D)$ is different from the always increasing trend of $P(C)$. This trend of $P(NC \cap D)$ becomes clear by looking at components of Eq. (6).At small $S_a(T, 5\%)$ values the probability of demolition, quantified by $F_{\theta_{r,D}}$, is close to zero because the residual story drift ratio (θ_r) values are negligible (i.e., $F_{\theta_{r,D}}(\theta_r) \approx 0$). As a result $P(NC \cap D)$ becomes negligible at small $S_a(T, 5\%)$ values. The probability of non-collapse, quantified by $\bar{F}_{IM_{C,l}}$, is close to zero at large $S_a(T, 5\%)$ values for all ground motion records. As a result, $P(NC \cap D)$ becomes negligible at large $S_a(T, 5\%)$ values. Therefore, the increasing and then decreasing trend of $P(NC \cap D)$ with increasing $S_a(T, 5\%)$ is due to the multiplication of two components; one that increases and another that decreases with increase of $S_a(T, 5\%)$. At $S_a(T, 5\%)$ values where probability of non-collapse and probability of demolition are not negligible, $P(NC \cap D)$ has non-zero values. At these $S_a(T, 5\%)$ values the increasing part of the $NC \cap D$ fragility is more affected by $F_{\theta_{r,D}}$ as $\bar{F}_{IM_{C,l}}$ is close to 1; and the decreasing part of the $NC \cap D$ fragility is more affected by $\bar{F}_{IM_{C,l}}$ as $F_{\theta_{r,D}}$ is close to 1.

When the building is not collapsed and the induced damage does not require the demolition of the building, structural and non-structural component damage scenarios become relevant. In this paper damage to bracing members of the SCBF system are considered. Fragilities for the damage scenarios including brace damage can be developed for each bracing member. As stated previously, three brace DS corresponding to no repair action (NR), brace straightening (BS), and brace replacement (BR) are considered for a bracing member. Three damage scenarios are created using these brace damage states: (i) $NC \cap ND \cap NR$; (ii) $NC \cap ND \cap BS$; and (iii) $NC \cap ND \cap BR$. The fragilities for these three brace damage scenarios are shown in Fig. 7 for the 3rd story right side brace.

It can be seen in Fig. 7 that the probability of no collapse and no demolition of the building without the need to repair the 3rd story right side brace (i.e. $P(NC \cap ND \cap NR)$) decreases and becomes small at $S_a(T, 5\%) \approx$ 1.5g. The probability of no collapse and no demolition but having to straighten the 3rd story right side brace (i.e., $P(NC \cap ND \cap BS)$) increases to about 25% at $S_a(T, 5\%) \approx 0.9$g and then decreases to nearly zero at $S_a(T, 5\%) \approx$ 2g. The probability of no collapse and no demolition but having to replace the 3rd story right side brace (i.e. $P(NC \cap ND \cap BR)$) increases to about 40% at $S_a(T, 5\%) \approx 1.4g$ and then becomes nearly zero at $S_a(T, 5\%) \approx 3g$. The $NC \cap ND \cap BS$ and $NC \cap ND \cap BR$ damage scenarios have a considerable probability at the MCE hazard level (where $S_a(T = 1.01sec., 5\%) = 0.89g$). The $NC \cap ND$ fragility is also shown in Fig. 7. The sum of $P(NC \cap ND \cap NR)$, $P(NC \cap ND \cap BS)$, and $P(NC \cap ND \cap BR)$ at each $S_a(T, 5\%)$ value is equal to $P(NC \cap ND)$ due to the mutual exclusiveness and collective exhaustiveness of the brace DS.

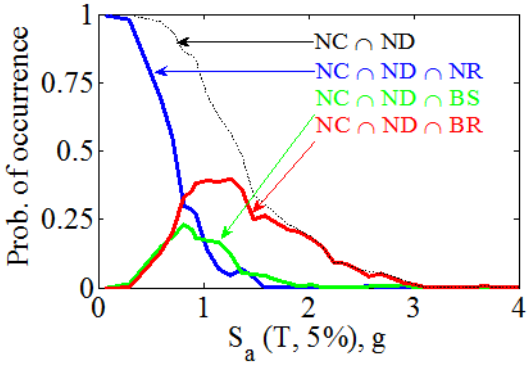

Fig. 7 Third story right side brace damage scenario fragilities

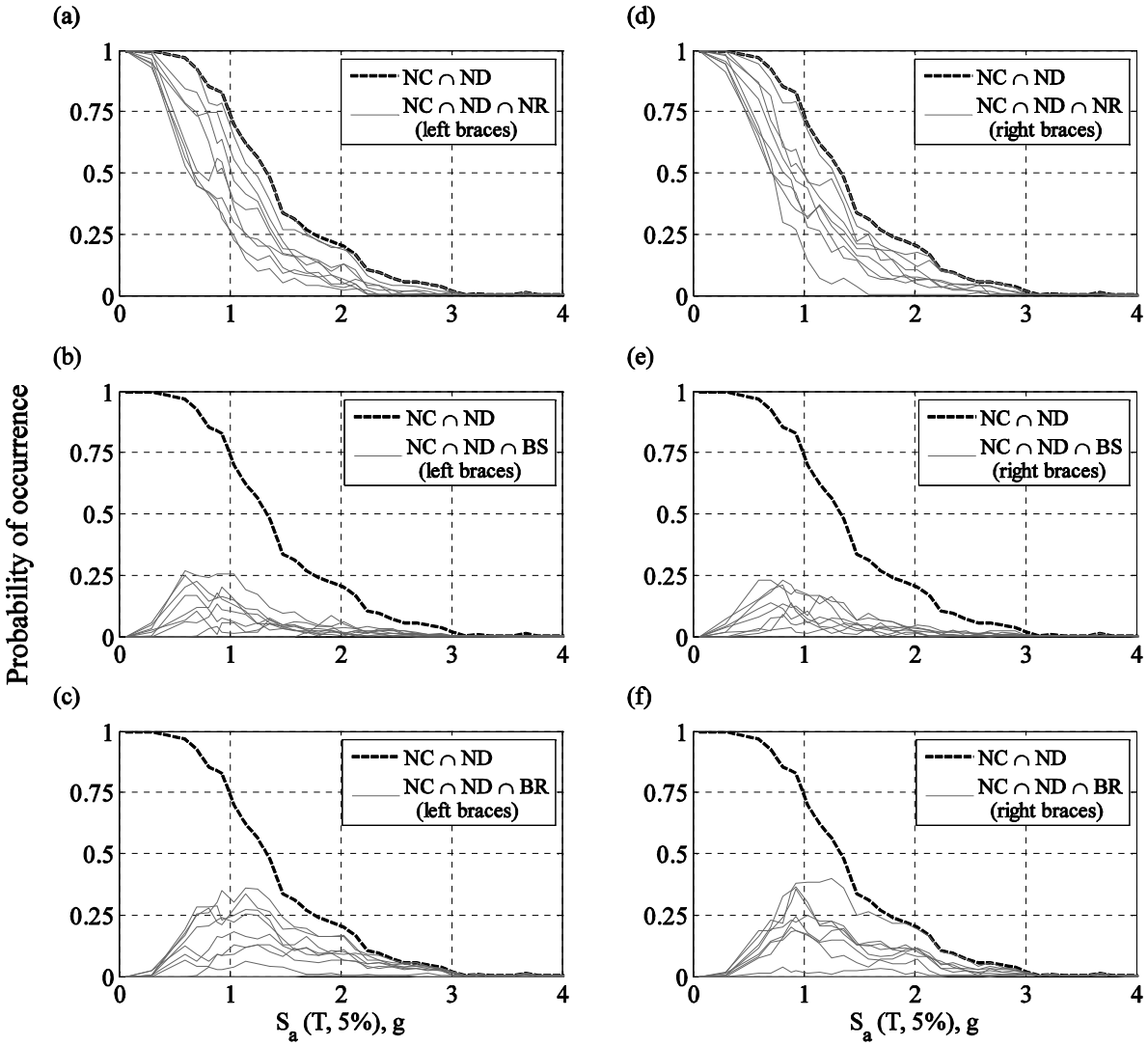

Fig. 8 Damage scenario fragility results for all braces: (a) $NC \cap ND \cap NR$ for left side braces; (b) $NC \cap ND \cap BS$ for left side braces; (c) $NC \cap ND \cap BR$ for left side braces; (d) $NC \cap ND \cap NR$ for right side braces; (e) $NC \cap ND \cap BS$ for right side braces; and (f) $NC \cap ND \cap BR$ for right side braces

Similar damage scenario fragility results can be constructed for other braces of the 9-story SCBF. Fig. 8 shows the $NC \cap ND \cap NR$, $NC \cap ND \cap BS$, and $NC \cap ND \cap BR$ fragilities for all 18 braces of the 9-story SCBF. The $NC \cap ND$ fragility is also shown in Fig. 8. Among the $NC \cap ND \cap NR$ fragilities shown in Fig. 8(a) and Fig. 8(d), those that are closer to the $NC \cap ND$ fragility correspond to braces with less damage. Among the $NC \cap ND \cap BS$ and $NC \cap ND \cap BR$ fragilities, the smallest fragilities, closer to the $S_a(T, 5\%)$ axis represent less damage. The $NC \cap ND \cap BS$ fragilities reach a peak at approximately near the DBE hazard level (where, $S_a(T = 1.01sec., 5\%) = 0.59g$), while the $NC \cap ND \cap BR$ fragilities reach a peak at approximately near the MCE hazard level (where, $S_a(T = 1.01sec., 5\%) = 0.89g$). The 9th story braces did not have any damage and thus the $NC \cap ND \cap NR$ fragilities for the 9th story braces are identical to the $NC \cap ND$ fragility. The 8th story brace damage is small for most GM, and the $NC \cap ND \cap NR$ fragilities for the 8th story braces are close to the $NC \cap ND$ fragility. The 3rd story braces are the most heavily damaged braces for most GM, and the $NC \cap ND \cap NR$ fragilities for the 3rd story braces are farthest from the $NC \cap ND$ fragility.

4 Conclusion

This paper presents damage scenario tree analysis (DSTA) for building seismic damage. A DSTA organizes the damage analysis of a building into system, subsystem, and component level damage assessments. Collapse and non-collapse of the building are the two damage states (DS) considered for the system level damage assessment. Demolition and reconstruction and non-demolition of the building are the repair actions corresponding to two DS considered at the subsystem level damage assessment. At the component level, different DS can be considered depending on the type of component. Various damage scenarios are developed using these damage states.

Three damages scenarios of interest, presented in this paper are: (i) collapse (C); (ii) non-collapse with demolition ($NC \cap D$); and (iii) non-collapse, non-demolition, with component damage ($NC \cap ND \cap DS_c$). The different DS considered for each damage assessment level are mutually exclusive and collectively exhaustive. Therefore, the damage scenarios considered by the DSTA for any individual component, are also mutually exclusive and collectively exhaustive. As a result, a DSTA provides a rigorous framework for calculating the fragilities for various damage scenarios.

The uncertainty corresponding to the evaluating DS probabilities is included through probabilistic DS fragility functions. The variability in structural response to different ground motion records is also considered on a record-by-record basis.

5 References

[1] F. Zareian, "Simplified performance-based earthquake engineering," PhD dissertation, Department of Civil and Environmental Engineering, Stanford University, Stanford, CA, 2006.

[2] J. Moehle and G. G. Deierlein, "A framework methodology for performance-based earthquake engineering," in *13th World conference on earthquake engineering*, Vancouver, BC, Canada, 2004.

[3] C. M. Ramirez and E. Miranda, "Significance of residual drifts in building earthquake loss estimation," *Earthquake Engineering & Structural Dynamics,* vol. 41, no. 11, pp. 1477-1493, 2012.

[4] FEMA, "Quantification of Building Sismic Performance Factors," Federal Emergency Management Agency, FEMA P695, Washington, DC, 2009.

[5] D. Vamvatsikos and C. A. Cornell, "Incremental Dynamic Analysis," *Earthquake Engineering & Structural Dynamics,* vol. 31, no. 3, pp. 491-514, 2002.

[6] E. Rosenblueth and R. Meli, "The 1985 earthquake: causes and effects in Mexico City," *Concrete International,* vol. 8, no. 5, pp. 23-34, 1986.

[7] K. Kawashima, "Seismic design and retrofit of bridges," in *Proceedings of the Twelfth World Conference on Earthquake Engineering*, Auckland, 2000.

[8] C. Christopoulos, S. Pampanin and M. N. Priestley, "Performance-based seismic response of frame structures including residual deformations. Part I: Single-degree of freedom systems," *Journal of Earthquake Engineering,* vol. 7, no. 1, pp. 97-118, 2003.

[9] K. Kawashima, G. A. MacRae, J.-i. Hoshikuma and K. Nagaya, "Residual displacement response spectrum," *Journal of Structural Engineering,* vol. 124, no. 5, pp. 523-530, 1998.

[10] G. A. MacRae and K. Kawashima, "Post-Earthquake Residual Displacement of Bilinear Oscillators," *Earthquake engineering & structural dynamics,* vol. 26, no. 7, pp. 701-716, 1997.

[11] S. A. Mahin and V. V. Bertero, "An evaluation of inelastic seismic design spectra," *Journal of the Structural Division,* vol. 107, no. 9, pp. 1777-1795, 1981.

[12] S. Pampanin, C. Christopoulos and M. N. Priestley, "Performance-based seismic response of frame structures including residual deformations. Part II: Multi-degree of freedom systems," *Journal of Earthquake Engineering,* vol. 7, no. 1, pp. 119-147, 2003.

[13] J. Ruiz-García and E. Miranda, "Evaluation of residual drift demands in regular multi-storey frames for performance-based seismic assessment," *Earthquake engineering & structural dynamics,* vol. 35, no. 13, pp. 1609-1629, 2006a.

[14] C. B. Haselton, "Assessing seismic collapse safety of modern reinforced concrete moment frame buildings," PhD Diss., Department of Civil and Environmental Engineering, Stanford University, Stanford, CA, 2006.

[15] S. R. Uma, S. Pampanin and C. Christopoulos, "Development of probabilistic framework for performance-based seismic assessment of structures considering residual deformations," *Journal of Earthquake Engineering,* vol. 14, no. 7, pp. 1092-1111, 2010.

[16] FEMA, "Seismic performance assessment of buildings, Volume 1, Methodology, FEMA P-58," Federal Emergence Management Agency, Washington, DC, 2012.

[17] C. A. Ericson, Hazard analysis techniques for system safety, Fredericksburg, VA: John Wiley & Sons, 2005.

[18] FEMA, "State of art report on performance prediction and evaluation of steel moment-frame buildings," Federal Emergency Management Agency, Report No. FEMA-355F, Washington, DC, 2000.

[19] D. Vamvatsikos, "Seismic performance uncertainty estimation via IDA with progressive accelerogram-wise latin hypercube sampling," *Journal of Structural Engineering,* vol. 140, no. 8, p. A4014015, 2014.

[20] ASCE, "Minimum Design Loads for Buildings and Other Structures," ASCE/SEI 7-10, Reston, Virginia, 2010.

[21] F. McKenna, "Object-oriented finite element programming: frameworks for analysis, algorithms and parallel computing," PhD dissertation, University of California at Berekeley, Berekeley, California, 1997.

[22] P. Uriz, F. C. Filippou and S. A. Mahin, "Model for Cyclic Inelastic Buckling of Steel Braces," *Journal of Structural Engineering,* vol. 134, no. 4, pp. 619-628, 2008.

[23] P. Uriz, "Toward Earthquake-Resistant Design of Concentrically Braced Steel-Frame Structures," PhD Diss., University of California at Berkeley, Berkeley, California, 2005.

[24] G. Akbas, "Probabilistic Earthquake Structural Damage Assessment of Steel Special CBF and Steel Self-Centering CBF Buildings," Thesis, Department of Civil and Environmental Engineering, Lehigh University, Bethlehem, PA, 2012.

[25] J. A. Powell, "Evaluation of special concentrically braced frames for improved seismic performance and constructability," PhD dissertation, University of Washington, Seattle, WA, 2010.